Japanese Journal of Applied Physics **51** (2012) 05EA01 **REGULAR PAPER**
DOI: 10.1143/JJAP.51.05EA01

Conformal Copper Coating of True Three-Dimensional Through-Holes Using Supercritical Carbon Dioxide

Mitsuhiro Watanabe*, Yuto Takeuchi, Takahiro Ueno, Masahiro Matsubara, Eiichi Kondoh, Satoshi Yamamoto[1], Naohiro Kikukawa[1], and Tatsuo Suemasu[1]

Interdisciplinary of Graduate School of Medicine and Engineering, University of Yamanashi, Kofu 400-8511, Japan
[1]*Electron Device Laboratory, Fujikura Ltd., Sakura, Chiba 285-8550, Japan*

Received October 15, 2011; revised January 24, 2012; accepted February 21, 2012; published online May 21, 2012

Copper thin films were deposited inside true three-dimensional, high aspect ratio, and complex shaped through-holes that were formed in glass substrates. The deposition was carried out in a supercritical carbon dioxide solution from a copper complex via hydrogen reduction. The conformal thin films were successfully deposited on the sidewalls of straight, crank-shaped, and Y-shaped through-holes. The coating length increased with decreasing the deposition temperature. Numerical simulations suggested an importance of the presence of a fluid motion in the through-holes.
© 2012 The Japan Society of Applied Physics

1. Introduction

Cu thin film deposition in high aspect ratio through-holes is a key issue in fabricating new generation through-silicon vias and through-glass vias for three-dimensional (3D) chip stacking. Flexible chip design will require complex shaped through-hole interconnections instead of traditional through-holes perpendicular to the substrate surface.[1] Several deposition techniques, such as electrochemical deposition (ECD),[2–5] physical vapor deposition (PVD),[6–8] and chemical vapor deposition (CVD),[7,9–16] have been attempted so far. However, ECD and PVD are inappropriate for coating inside the high aspect ratio through-holes due to their poor step coverage. CVD is a well-known technique for the deposition of high aspect ratio through-holes. However, its deposition rate is relatively low and its applicability to complex shaped through-holes is not clear.

Recently, the deposition technique using supercritical fluids, where supercritical CO_2 is commonly used, have been attracted extensive attention.[17–24] The CO_2 has a critical temperature of 304.2 K and a critical pressure of 7.28 MPa of which condition can be more easily achieved than other substances.[25] The supercritical CO_2 behaves as both a gas and a liquid and has many unique properties, such as zero surface tension, low viscosity and excellent diffusivity like a gas, and high density and solvent capability like a liquid. It was demonstrated that supercritical fluid deposition techniques are capable of filling nanometer-sized features with metals.[17,18,26–33] For these reasons, it is now expected that the Cu coating the inside walls of high aspect ratio and complex shaped holes can be achieved by using the supercritical CO_2.

In the present study, we used supercritical CO_2 to deposit a conformal Cu thin film inside the true 3D through-holes having different complex shapes.

2. Experimental Procedure

A schematic illustration of the experimental set-up is shown in Fig. 1. In the present study, a flow-type reaction system[24] was used. The liquid CO_2 was pressurized at a pressure higher than the critical pressure of CO_2 (7.28 MPa[25]) with a high pressure pump. The preheater was heated to 423 K, and the reactor was heated to a temperature higher than the critical temperature of CO_2 (304.2 K[25]) with heating mantles. The low-pressure H_2 gas was mixed in the supercritical CO_2 fluid with a gas mixing unit. Acetone, which is an auxiliary solvent dissolving the precursor, was injected into the supercritical CO_2 fluid. This fluid was then preheated by the preheater and was supplied to the reactor placed in the heating mantle. The pressure of the reactor was adjusted with a back-pressure regulator. The gas mixing unit, the preheating system, the reactor, and other related piping and valves were maintained at 313 K in a thermostatic chamber. The substrate was fixed facedown on the reactor wall.

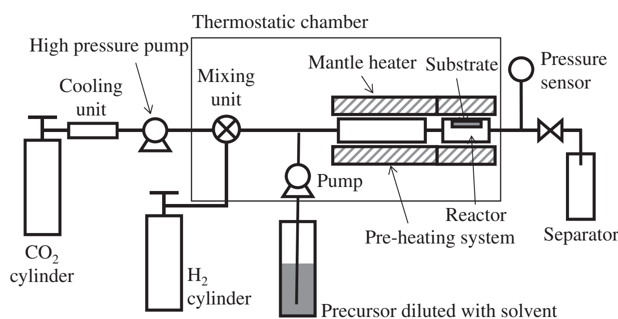

Fig. 1. Schematic illustration of the supercritical CO_2 deposition apparatus used in the present study.

Cu-bis(diisobutyrylmethanate) [$Cu(dibm)_2$] was used as the precursor. Material of the substrate was glass. In the substrates, differently shaped through-holes, namely straight, crank-shaped, and Y-shaped through-holes, were formed as shown in Fig. 2. The aspect ratio of the straight, crank-shaped, and Y-shaped through-holes is 10.3, 10.3, and 7.0, respectively. Femtosecond laser irradiation and wet chemical etching were used for fabricating the crank- and Y-shaped through-holes in the substrates. Detailed fabricating techniques of these complex shaped through-holes were given by ref. 1. The deposition conditions are summarized in Table I. The substrate was fixed using two arrangements. In one arrangement, a substrate was fixed to the sidewall of the reactor. In another arrangement, a substrate was placed about 1 mm apart from the sidewall of the reactor. These arrangements are called hereafter the "contact arrangement" and the "float arrangement", respectively.

*E-mail address: mitsuhirow@yamanashi.ac.jp

 © 2012 The Japan Society of Applied Physics

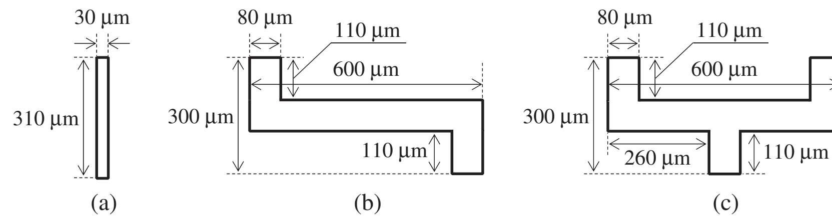

Fig. 2. Schematic diagrams of the shapes of through-holes. (a) Straight hole. (b) Crank-shaped hole. (c) Y-shaped hole.

Table I. Deposition conditions.

Deposition temperature (K)	493, 513, 553
Pressure (MPa)	10
Deposition time (min)	60, 240, 480
CO_2 flow rate (10^{-3} mol·min^{-1})	77.5, 221.5
H_2 concentration (mol%)	1.53
Cu(dibm)$_2$ concentration (10^{-3} mol%)	29.2
Acetone concentration (%)	5.2 (in CO_2)

After the Cu deposition, the samples were characterized using optical microscopy and scanning electron microscopy (SEM). The samples for cross-sectional observation using microscopy were prepared by using a mechanical polishing and a cross-section polishing. Plan view observations were also carried out using a transmitted light after removing the Cu thin films deposited at the substrate surface. The film thicknesses were measured with a surface profilometer (DEKTAK).

In order to understand the deposition phenomena occurring in the through-hole, numerical simulations were performed by using a conventional thermo-fluid analysis software ANSYS CFX based on the finite volume method. The through-hole was modeled to consist of triangular pyramid shaped meshes. The physical properties of the materials used for numerical simulation were shown in Table II. Temperature dependence of the density ρ (kg·m^{-3}), the viscosity coefficient C_v (Pa·s), and the thermal conductivity C_t (W·m^{-1}·K^{-1}), of the CO_2 was expressed by

Table II. Physical properties of each material.

CO_2	Molar mass (kg·kmol^{-1})	44
	Specific heat capacity (J·kg^{-1}·K^{-1})	1178.38
Cu(dibm)$_2$	Molar mass (kg·kmol^{-1})	373.9

$$\rho = D_0 + D_2(T - D_1) + D_3(T - D_1)^2, \quad (1)$$

$$C_v = aT + b, \quad (2)$$

$$C_t = cT + d, \quad (3)$$

where D_0, D_1, D_2, D_3, a, b, c, and d are appropriately-defined coefficients and T is temperature. In the present study, the values of D_0, D_1, D_2, and D_3 in the eq. (1) are used 122 kg·m^{-3}, 473 K, -0.391 kg·m^{-3}·K^{-1}, and 1.56×10^{-3} kg·m^{-3}·K^{-2}, respectively. In case of the calculation of the viscosity coefficient, the values of a and b in the eq. (2) were used 3.37×10^{-8} Pa·s·K^{-1} and 8.57×10^{-6} Pa·s, respectively. Also, in case of the calculation of the thermal conductivity, the values of c and d in the eq. (3) were used 6.57×10^{-5} W·m^{-1}·K^{-2} and 4.54×10^{-3} W·m^{-1}·K^{-1}, respectively. The specific heat capacity, the density, the viscosity coefficient, and the thermal conductivity of the Cu(dibm)$_2$ used a value same as the CO_2 each because molar density of the Cu(dibm)$_2$ was extremely lower than that of the CO_2.

The distribution of the Cu precursor in the CO_2 fluid was also analyzed in the simulations. The mass concentration of the Cu(dibm)$_2$ was used a value of 6.5×10^{-4} which estimated from the mass flow rate of all materials. As a boundary condition, the consumption rate of the Cu precursor at the sidewall of the through-hole was set by using the following Langmuir–Hinshelwood type surface reaction rate:[24)]

$$G(C) = 8.26 \times 10^6 \exp\left(-\frac{3990}{T}\right) \frac{63.4 \exp\left(\frac{1850}{T}\right) C \sqrt{4040 \exp\left(-\frac{6250}{T}\right) C_{H_2}}}{\left(1 + 63.4 \exp\left(\frac{1850}{T}\right) C + \sqrt{4040 \exp\left(-\frac{6250}{T}\right) C_{H_2}}\right)^2}, \quad (4)$$

$$R_c = \frac{G(C) \times 10^{-9} \times 8.92 \times 10^3}{60}, \quad (5)$$

where $G(C)$ is deposition rate of the Cu (in nm·min^{-1}), C and C_{H_2} are molar fractions of the Cu precursor and H_2 gas for the all materials flowed in the through-hole, and R_c is consumption rate of the Cu(dibm)$_2$ (in kg·m^{-2}·s^{-1}).

3. Results and Discussion

3.1 Coating characterization of Cu in straight through-holes

Figures 3(a) to 3(c) show cross-sectional optical micrographs of Cu thin films deposited in the straight through-holes at different deposition temperatures with the contact arrangement. The deposition of the Cu thin films occurred at the surfaces of the substrate as well as the hole sidewalls at any temperatures employed in this study. The temperature dependence of the coating length of the Cu thin films was observed, where the coating length increased with decreasing deposition temperature. At a lower temperature of 493 K [Fig. 3(a)], the thickness of the Cu thin film seemed almost constant over the hole length. At a medium temperature of 513 K [Fig. 3(b)], the Cu thin films showed an inhomoge-

 © 2012 The Japan Society of Applied Physics

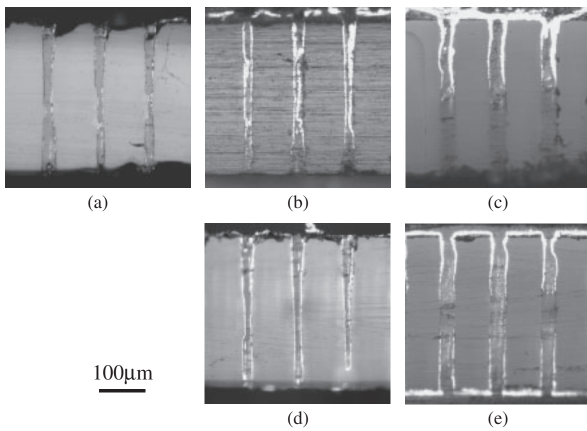

Fig. 3. Cross-sectional optical micrographs of the straight through-holes lined with Cu thin films. The Cu thin films were deposited at (a) 493, (b) 513, and (c) 553 K with the contact arrangement and at (d) 513 and (e) 553 K with the float arrangement.

neous thickness distribution and the coating length decreased to approximately 250 μm. At a higher temperature of 553 K [Fig. 3(c)], the Cu thin films were formed from the top to a length of approximately 150 μm of the holes. The coating depth is considered to depend on balance between consumption rate and diffusion capability of the precursor. These tendencies suggest that the Cu precursor was consumed at the top of the holes and become deficient at a deep part of the holes when the temperature was high. On the other hand, at a lower temperature, the Cu precursor reached the bottom of the holes, because the low consumption of the precursor allowed good diffusion transport of the precursor.

Figures 3(d) and 3(e) show cross-sectional optical micrographs of Cu thin films deposited in the straight through-holes at different deposition temperatures with the float arrangement. At a lower temperature of 513 K [Fig. 3(d)], the Cu film was coated with a constant thickness over the hole sidewalls. At a higher temperature of 553 K [Fig. 3(e)], the Cu thin film was also formed over the hole sidewalls but a clear decrease in the thickness was observed at the center of the hole length. These results indicate that the Cu precursor was transported from either the top or the bottom of the hole when the float arrangement was employed. It is obvious that the float arrangement resulted in a better conformability than the contact arrangement because the float arrangement allows the supply of the precursor from the both ends of the holes and thus the apparent aspect ratio is halved.

3.2 Cu coating of high aspect ratio and complex shaped through-holes

3.2.1 Thickness distribution along the hole length

Figure 4 shows top view transmission optical micrographs of the crank- and Y-shaped through-holes before [Figs. 4(a) and 4(b)] and after the Cu deposition [Figs. 4(c) to 4(h)]. In these micrographs, the dark parts show the presence of Cu at the hole sidewalls obviously because thick Cu does not transmit a light. The arrows in these figures indicate brighter parts which has thinner Cu. When the Cu was deposited at a temperature of 513 K and a CO_2 flow rate of 77.5 × 10^{-3} mol/min by using the contact arrangement [Figs. 4(c) and 4(d)], the dark high contrast part extends from the top to

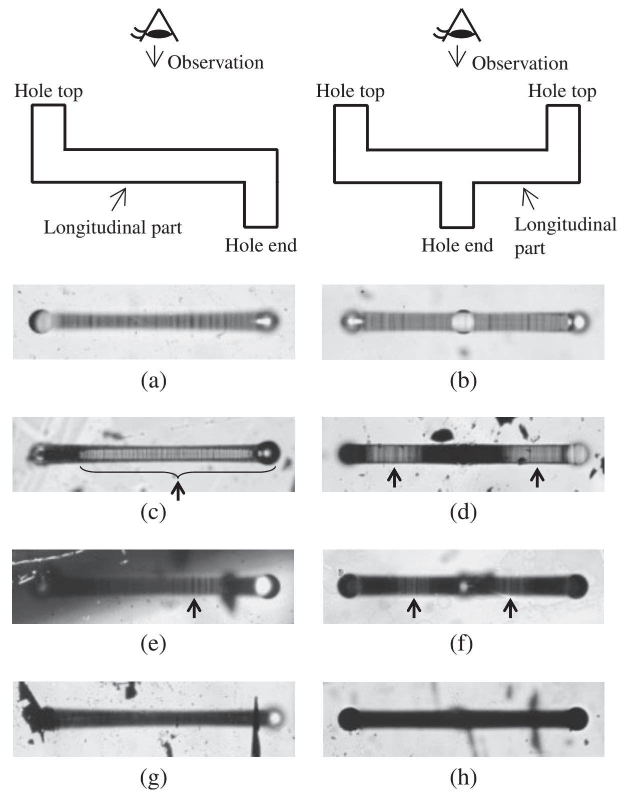

Fig. 4. Top-view transmission optical micrographs of (a, c, e, g) the crank-shaped and (b, d, f, h) the Y-shaped through-holes. (a, b) Before the Cu deposition. (c, d) The Cu thin films were deposited at a temperature of 513 K and a CO_2 flow rate of 77.5 × 10^{-3} mol/min by using the contact arrangement. (e, f) The Cu thin films were deposited at a temperature of 553 K and a CO_2 flow rate of 221.5 × 10^{-3} mol/min by using the contact arrangement. (g, h) The Cu thin films were deposited at a temperature of 553 K and a CO_2 flow rate of 221.5 × 10^{-3} mol/min by using the float arrangement.

a longitudinal part close to the corner of the hole, but the longitudinal parts showed a weaker contrast. In other words, the Cu thin films were formed from the top to the corner part of the hole (aspect ratio: approximately 2.4) but did not cover the whole length (aspect ratio: 10.3 for the crank-shaped hole and 7.0 for the Y-shaped hole).

In order to investigate the effect of the flow rate of the fluids, the CO_2 flow rate was increased to 221.5 × 10^{-3} mol/min. In the case of the contact arrangement, the length of the dark part increased but the contrast was not uniform [Figs. 4(e) and 4(f)]. Figures 4(g) and 4(h) show the samples deposited by using the float arrangement. Obviously, a good strong contrast is seen for the whole length, indicating a good longitudinal distribution of a thick Cu film.

Figure 5 shows cross-sectional images of a crank-shaped through-hole deposited by using the float arrangement. Figure 5(a) is an optical micrograph of the hole and Figs. 5(b) to 5(f) are SEM images of the Cu thin film obtained at the positions of B to F in Fig. 5(a), respectively. It is seen that the Cu thin film completely coated the hole sidewall. We obtained the same observations on the Y-shaped through-holes. Figure 6 shows thickness distribution of the Cu thin films determined from SEM images. The thickness of the Cu thin film formed inside the hole sidewall was approximately 200 nm and this value was close to that

 © 2012 The Japan Society of Applied Physics

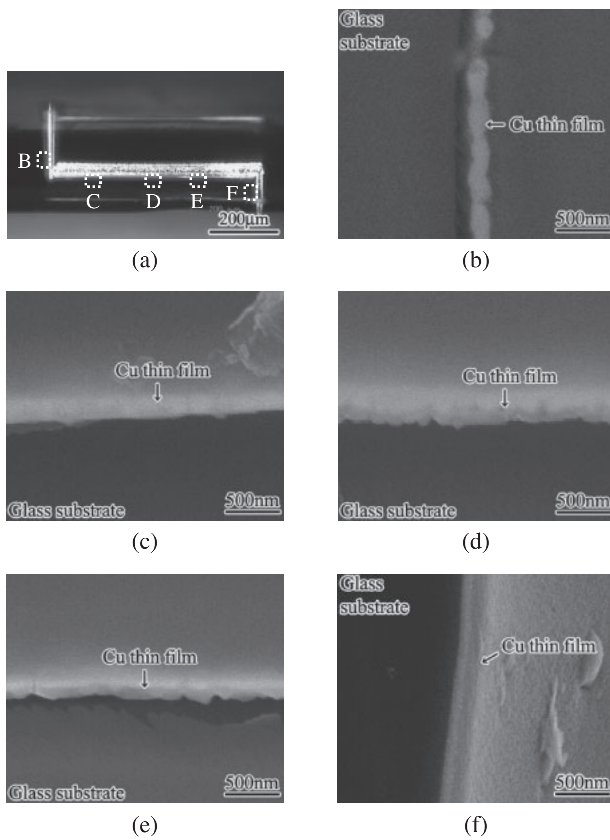

Fig. 5. Cross-sectional images of the crank-shaped through-hole deposited at a temperature of 553 K and a CO_2 flow rate of 221.5×10^{-3} mol/min by using the float arrangement. (a) Full optical view of a through-hole cross-section. (b)–(f) SEM images of the Cu thin film obtained at the position of B to F in (a), respectively.

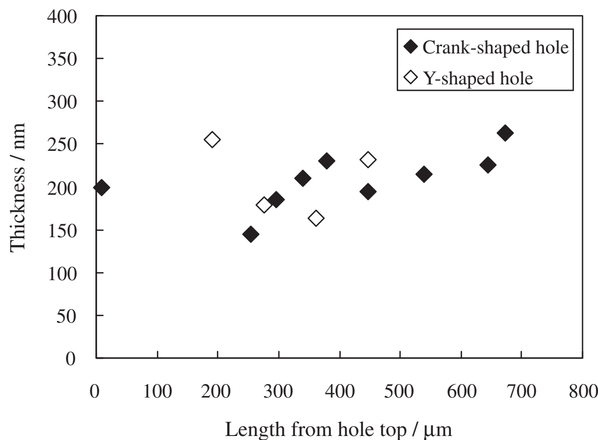

Fig. 6. Relationship between the length from the top of the through-hole and thickness of the Cu thin film.

formed on the substrate surface (200 nm). From these SEM observations, we can conclude that conformal Cu coating of the sidewalls of high aspect ratio and complex shaped through-holes was succeeded.

3.2.2 Numerical study on thickness distribution

The increase of flow rate with the float arrangement [Figs. 4(g) and 4(h)] resulted in a better coating performance for the high aspect ratio and complex shaped through-holes. A small spacing (1 mm) was thought to induce a difference

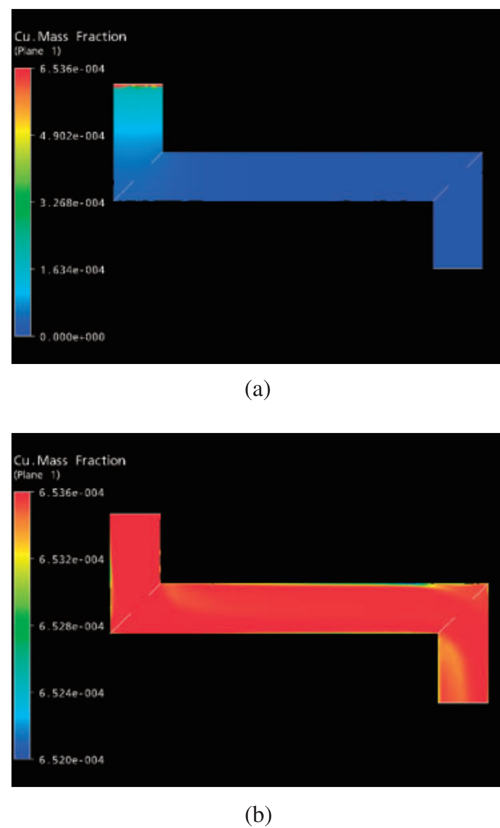

Fig. 7. (Color) Cu concentration distributions in the crank-shaped through-hole at a temperature of 513 K and fluid flow rates of (a) 0.0001 and (b) 10 m/s.

in the flow rate between the upper and lower surfaces so as to produce the fluid motion inside the holes.

In order to investigate the effects of the fluid flow on the Cu coating in the complex shaped through-hole, numerical fluid flow dynamics simulations were carried out. In these simulations, the motion of the CO_2 fluid and the concentration distributions of the Cu in the hole were analyzed. Figure 7 shows the Cu concentration distributions in the crank-shaped through-hole at fluid flow rates of (a) 0.0001 and (b) 10 m/s at 513 K. When the fluid flow rate was nearly zero [0.0001 m/s, Fig. 7(a)], the Cu precursor was consumed at the top of the hole and was hardly transported deep in the hole. In contrast to that, at the fluid flow rate of 10 m/s, the Cu precursor was reached to the hole end as shown in Fig. 7(b). Comparing two fluid flow rate conditions, it is found that the presence of the fluid motion (advection) eases the Cu precursor to be transported from the hole top to the hole end.

Figure 8 shows the numerical results on the thickness distribution of the Cu thin film inside the crank- and Y-shaped through-holes. At a fluid flow rate of 0.0001 m/s, the Cu thin films were formed near the hole top whereas the thickness decreased abruptly. Obviously, the Cu precursor does not reach the hole end. At a fluid flow rate higher than 0.001 m/s, the Cu thin film distributed from the hole top to the hole end. The thickness of the Cu thin film decreased more moderately with increasing length than the previous case. At a much higher fluid flow rate more than 1 m/s, the Cu thin film having a constant thickness distribution was formed over the whole hole length. These results indicate

 © 2012 The Japan Society of Applied Physics

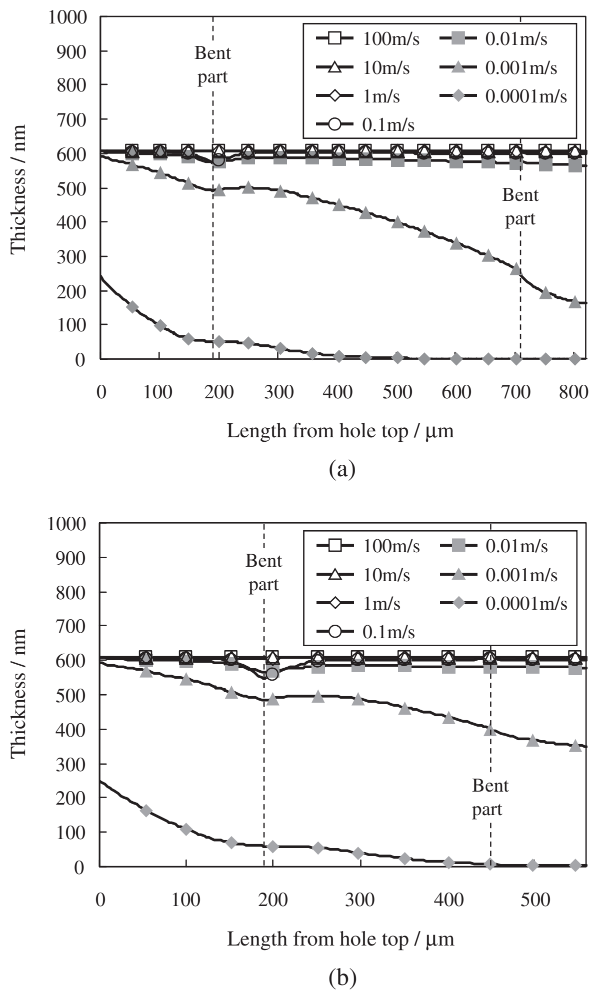

Fig. 8. Numerical results on thickness distribution of the Cu thin film deposited inside (a) the crank-shaped and (b) Y-shaped through-holes.

that conformal Cu coating inside the high aspect ratio and complex shaped through-holes can be achieved when the fluid motion through the holes exists.[34] Therefore, it is possible that the fluid motion existed inside the through-hole when the float arrangement was used.

4. Conclusions

Cu coating inside the high aspect ratio and complex shaped through-holes was carried out using the supercritical CO_2 and the following findings were obtained.

(1) Cu thin films were successfully deposited on the sidewalls of straight, crank-shaped, and Y-shaped through-holes opened in the glass substrates by using the supercritical CO_2 deposition technique.

(2) The coating length increased with decreasing deposition temperature. This is because low consumption of the precursor allowed good diffusion transport of the precursor.

(3) Conformal Cu coating of the sidewalls of the crank- and Y-shaped through-holes was achieved under a high flow rate condition by using the float arrangement. Numerical simulations indicate that the conformal Cu coating is due to the difference of the flow rates between the upper and reverse substrate sides.

1) S. Yamamoto, O. Nukaga, H. Wakioka, T. Suemasu, and H. Hashimoto: Denki Gakkai Ronbunshi E **129** (2009) 14 [in Japanese].
2) O. Cavalleri, S. E. Gilbert, and K. Kern: Surf. Sci. **377–379** (1997) 931.
3) O. Voigt, B. Davepon, G. Staikov, and J. W. Schulze: Electrochem. Acta **44** (1999) 3731.
4) D. K. Gebregziabiher, Y. G. Kim, C. Thambidurai, V. Ivanova, P. H. Haumesser, and J. L. Stickney: J. Cryst. Growth **312** (2010) 1271.
5) S. Armini, Z. Tokei, H. Volders, Z. El-Mekki, A. Radisic, G. Beyer, W. Ruythooren, and P. M. Vereechen: Microelectron. Eng. **88** (2011) 754.
6) B. Navinšek, P. Panjan, and I. Milošev: Surf. Coatings Technol. **116–119** (1999) 476.
7) M. Proust, F. Judong, J. M. Gilet, L. Liauzu, and R. Madar: Microelectron. Eng. **55** (2001) 269.
8) M. Gossia and W. N. Shafarman: Thin Solid Films **480–481** (2005) 33.
9) S. Chichibu, N. Yoshida, H. Higuchi, and S. Matsumoto: Jpn. J. Appl. Phys. **31** (1992) L1778.
10) J. A. T. Norman, D. A. Roberts, A. K. Hochberg, P. Smith, G. A. Petersen, J. E. Parmeter, C. A. Apblett, and T. R. Omstead: Thin Solid Films **262** (1995) 46.
11) G. Friese, A. Abdul-Hak, B. Schwierzi, and U. Höhne: Microelectron. Eng. **37–38** (1997) 157.
12) H. J. Jin, M. Shiratani, Y. Nakatake, T. Fukuzawa, T. Kinoshita, Y. Watanabe, and M. Toyofuku: Jpn. J. Appl. Phys. **38** (1999) 4492.
13) R. Kröger, M. Eizenberg, D. Cong, N. Yoshida, L. Y. Chen, S. Ramaswami, and D. Carl: Microelectron. Eng. **50** (2000) 375.
14) C. L. Chang, C. L. Lin, and M. C. Chen: Jpn. J. Appl. Phys. **43** (2004) 2442.
15) K. Takenaka, K. Koga, M. Shiratani, Y. Watanabe, and T. Shingen: Thin Solid Films **506–507** (2006) 197.
16) T. Momose, M. Sugiyama, E. Kondoh, and Y. Shimogaki: Jpn. J. Appl. Phys. **49** (2010) 05FF01.
17) J. M. Blackburn, D. P. Long, A. Cabañas, and J. Watkins: Science **294** (2001) 141.
18) E. Kondoh and H. Kato: Microelectron. Eng. **64** (2002) 495.
19) A. Cabañas, X. Shan, and J. J. Watkins: Chem. Mater. **15** (2003) 2910.
20) X. R. Ye, Y. Kin, C. Wang, and C. M. Wai: Adv. Mater. **15** (2003) 316.
21) E. T. Hunde and J. J. Watkins: Chem. Mater. **16** (2004) 498.
22) A. Cabañas, D. P. Long, and J. J. Watkins: Chem. Mater. **16** (2004) 2028.
23) E. Kondoh: Jpn. J. Appl. Phys. **44** (2005) 5799.
24) M. Matsubara, M. Hirose, K. Tamai, Y. Shimogaki, and E. Kondoh: J. Electrochem. Soc. **156** (2009) H443.
25) R. Span and W. Wagner: J. Phys. Chem. Ref. Data **25** (1996) 1509.
26) A. Cabañas, J. M. Blackburn, and J. J. Watkins: Microelectron. Eng. **64** (2002) 53.
27) E. Kondoh: Jpn. J. Appl. Phys. **43** (2004) 3928.
28) X. R. Ye, C. M. Wai, Y. Lin, J. S. Young, and M. H. Engelhard: Surf. Coatings Technol. **190** (2005) 25.
29) E. Kondoh and J. Fukuda: J. Supercrit. Fluids **44** (2008) 466.
30) T. Momose, M. Sugiyama, E. Kondoh, and Y. Shimogaki: Appl. Phys. Express **1** (2008) 097002.
31) E. Kondoh, K. Nagano, C. Yamamoto, and J. Yamanaka: Microelectron. Eng. **86** (2009) 902.
32) F. Kano, H. Uchida, and S. Koda: J. Supercrit. Fluids **50** (2009) 313.
33) E. Kondoh, M. Matsubara, K. Tamai, and Y. Shimogaki: Jpn. J. Appl. Phys. **49** (2010) 05FA07.
34) M. Matsubara and E. Kondoh: MRS Proc. **1156** (2009) 1156-D08-07-F06-07.

 © 2012 The Japan Society of Applied Physics